applied sciences

MDPI

Article

Distributed Robust Routing Optimization for Laser-Powered UAV Cluster with Temporary Parking Charging

Xunzhuo He, Yuanchang Zhong * and Han Li

School of Electrical Engineering, Chongqing University, Chongqing 400044, China; 202311021065@stu.cqu.edu.cn (X.H.); 202311131303@stu.cqu.edu.cn (H.L.)
* Correspondence: zyc@cqu.edu.cn

Abstract

Unmanned aerial vehicle (UAV) clusters are increasingly deployed in power system applications, such as transmission line inspection, fault diagnosis, and post-disaster emergency communication restoration. Nonetheless, limitations of range and battery capacity have rendered the assurance of uninterrupted task operation a critical concern. Efficient cooperation and energy replenishment solutions are crucial for effective UAV cluster scheduling to resolve this issue. This study proposes an innovative scheduling method that integrates UAV path planning with laser-based remote charging technology. Initially, a scheduling model incorporating both energy consumption and task completion time is established. Subsequently, an integrated laser-powered UAV model is proposed, unifying charging operations with mission execution processes. Furthermore, a distributed robust optimization (DRO) framework is proposed to handle spatiotemporal uncertainties, particularly those caused by weather conditions. Finally, the proposed scheduling method is applied to a disaster recovery scenario of a power system. Simulation results demonstrate that the proposed strategy significantly outperforms traditional scheduling methods without remote charging by achieving higher task completion rates and improved energy efficiency. These findings substantiate the effectiveness and engineering feasibility of the proposed method in enhancing UAV cluster operational capabilities under stringent energy constraints.

Keywords: laser-power UAV; remote charging; energy efficiency; distributed robust optimization

check for updates

Received: 13 August 2025
Revised: 27 August 2025
Accepted: 1 September 2025
Published: 2 September 2025

Citation: He, X.; Zhong, Y.; Li, H. Distributed Robust Routing Optimization for Laser-Powered UAV Cluster with Temporary Parking Charging. *Appl. Sci.* **2025**, *15*, 9676. https://doi.org/10.3390/app15179676

Copyright: © 2025 by the authors. Licensee MDPI, Basel, Switzerland. This article is an open access article distributed under the terms and conditions of the Creative Commons Attribution (CC BY) license (https://creativecommons.org/licenses/by/4.0/).

1. Introduction

In recent years, the deployment of unmanned aerial vehicle (UAV) clusters in power systems has grown increasingly prevalent, being extensively employed for critical functions such as transmission line inspections [1], fault diagnosis [2], and post-disaster emergency communication restoration [3]. Due to their exceptional mobility, small size, and multi-payload integration capabilities, UAV clusters can efficiently execute intricate aerial tasks. Especially in the post-disaster emergency communication recovery, UAVs provide an efficient solution for time-critical supply distribution in emergency response operations. Nevertheless, the constrained battery capacity limits the flying time of UAV clusters, hindering task continuity during extended tasks. Traditional solutions primarily depend on augmenting the quantity of UAVs or establishing stationary charging stations [4], which not only substantially escalates deployment costs but also constrains their feasibility in intricate terrain situations. Consequently, researchers are extensively concentrating on endurance challenges and task scheduling strategies for UAV clusters.

The endurance issue of UAVs can be addressed through recharging. The conventional charging method is swapping the batteries, wherein the UAV visits a charging station to replace the depleted battery with a fully charged one [5]. This manual battery switch method necessitates assistance, adversely impacting UAV operations and resulting in considerable service disruptions in remote regions, rendering it inappropriate for contemporary UAV cluster applications. In contrast to conventional charging techniques, wireless power transfer (WPT) technology provides enhanced safety, comfort, and flexibility to intricate surroundings owing to its non-contact energy transfer properties, rendering it a viable alternative for mitigating the endurance challenges of UAV clusters [6]. Among WPT technologies, laser charging stands out as an exceptionally suited alternative for in-flight energy replenishment of UAV clusters due to its high energy density, excellent beam directivity, and robust tolerance to external interference.

Preliminary research has already established the viability of laser charging. In 2003, NASA used a 940 nm, 500 W ground-based laser to illuminate a GaInP2 triple-junction solar cell on a UAV, facilitating 6 W power output and maintaining flight for 15 min [7]. In 2006, Kinki University in Japan accomplished a flight duration exceeding 1 h for an electric kite, utilizing a power transfer of 42 W and a system electro-optical conversion efficiency of 7.2% [8]. In 2009, Laser Motive Inc. successfully powered an ELICAN quadrotor UAV in a stationary state for 12.5 h, establishing a new endurance record [9]. In 2012, the business collaborated with Lockheed Martin to develop a compact UAV laser energy delivery system for U.S. Army Special Operations Forces [10]. In 2023, Nguyen et al. from Kyushu University, Japan, proposed a dynamic optical wireless power transfer (OWPT) system comprising a laser transmitter integrated with a tracking camera to enable continuous charging for electric vehicles (EVs) [11].

Building upon charging technology, the development of UAV cluster scheduling methods enables optimal energy utilization, thereby ensuring task completion efficiency.

The majority of studies on UAV scheduling strategies concentrate on optimizing the flight trajectories of individual UAVs while paying insufficient attention to the charging of UAV clusters during task execution. Current research on UAV cluster charging solutions, including mobile charging platform planning and charging sequence scheduling, typically isolates the charging process from task execution, thereby underutilizing their potential for collaboration. Moreover, prevailing scheduling methodologies, primarily designed for small-scale, short-duration operations, fail to adequately account for meteorological variability's critical impact on UAV flight time uncertainties. The main innovation of this paper lies in the integration of UAV path planning with laser-based remote charging technology. We propose a novel scheduling approach that jointly optimizes energy consumption and mission completion time. Furthermore, a distributed robust optimization framework is introduced to address uncertainties in flight time caused by weather disturbances.

This paper makes the following two contributions:

1. A UAV cluster scheduling model is proposed for communication restoration in the distribution network post-disaster by optimizing task allocation and execution pathways. This concept enhances the efficiency of UAV collaboration while accounting for energy limitations. Furthermore, we implemented laser charging technology to develop an effective charging-operation cluster scheduling model.
2. A distributed robust optimization (DRO) model is proposed that explicitly accounts for spatiotemporal meteorological uncertainty (e.g., rainfall, wind dynamics, and atmospheric disturbances) in long-range laser UAV operations. This model guarantees reliable task scheduling under weather-induced perturbations.

The subsequent sections of this work are structured as follows: Section 2 introduces relevant work research. Section 3 introduces the application of UAV scheduling and

the principle of laser charging. Section 4 develops a UAV cluster scheduling model for post-disaster distribution network load restoration, incorporating the benefits of laser charging and addressing flight time uncertainties. Section 5 presents simulation results and evaluates the performance of robust optimization under varying confidence intervals. Finally, Section 6 concludes the paper and outlines future research directions.

2. Related Work

In the domain of cooperative UAV scheduling, the integrated optimization of charging strategies and task allocation has emerged as a critical research focus aimed at enhancing overall system performance, with numerous scholars proposing innovative approaches from diverse perspectives. Hassija et al. introduced a game-theoretic scheduling algorithm for UAV charging inside a peer-to-peer network, designed to allocate constrained charging slots equitably and economically, taking into account task urgency and deadlines [12]. Zhao et al. examined collaborative computation offloading and charge scheduling in multi-UAV mobile edge computing networks, proposing a TD3-based strategy to enhance system utility [13]. Ref. [14] primarily examined last-mile delivery utilizing trucks and collaborating UAVs, suggesting schedule optimization for both single and multi-truck contexts to enhance delivery efficiency. Yang et al. [15] employed reinforcement learning for the real-time scheduling of tasks within a UAV cluster. By calculating task performance efficiency, the cluster of UAVs autonomously made behavioral judgments to enable a decentralized network. Jin et al. [16] evaluated the charging of a wireless rechargeable sensor network using a UAV. Charging deadlines for sensors and energy levels of UAVs were integrated into the charging system. A UAV scheduling model was developed to optimize the number of sensors charged by the UAV. An approximation algorithm was created to address the proposed model, and simulation results indicated that the suggested solution approach offered numerous advantages compared to the Greedy Replenished Energy Algorithm.

The evolution of UAV logistics systems has generated multiple methodological approaches to address coordination and efficiency challenges. Nguyen and Hà [17] investigated heavy-item transportation via cooperative communal UAVs, presenting a Mixed Integer Linear Programming (MILP) model and a metaheuristic to tackle synchronization and nonlinear power consumption. Their methodology demonstrated enhancements in efficiency. Poikonen and Golden [18] presented the notion of the Vehicle Routing Problem (VRP) with UAV in an early paper, analyzing several worst-case scenarios. But their research is confined to theoretical analysis and fails to provide a mathematical model or technique. As UAV scheduling research has progressed, researchers have transitioned from theoretical analysis to the creation of tangible mathematical models and technology solutions. VRP formulations considering single and multiple UAVs per truck were established in [19,20]. Joint transportation of commodities using vehicles and UAVs, aiming to meet schedule limitations while minimizing costs as the goal function. Deng et al. [21] developed a UAV-ground vehicle cooperative system for large-area coverage, featuring area partitioning, path optimization, and hybrid genetic-mathematical programming. Jung and Oh [22] developed a novel deep reinforcement learning framework featuring an attention mechanism to address single-UAV heterogeneous mission planning, which they formulated as a specialized vehicle routing problem. Li et al. [23] proposed the two-echelon vehicle routing problem with time windows and mobile satellites (2E-VRP-TM) framework, extending traditional vehicle routing problems to optimize synchronized van-UAV delivery operations with time windows and mobile satellite coordination.

Several optimization approaches have been proposed for UAV-assisted wireless communication systems to improve network coverage and capacity. Wu et al. [24] formulated

a joint trajectory and communication design problem for a UAV-enabled multiple access system, aiming to maximize the minimum user rate. The authors modeled the problem as a non-convex mixed-integer optimization and proposed an iterative algorithm based on block coordinate descent (BCD) and successive convex approximation (SCA) to obtain a high-quality suboptimal solution. Chowdhery and Jamieson [25] highlighted that emergency scenarios (e.g., natural disasters) can severely degrade wireless network performance, resulting in unmet user demand or coverage gaps. To address this challenge, the authors proposed the deployment of dynamically positioned UAV-mounted hotspots to augment network capacity. In their framework, an autonomous aerial hotspot serves a group of ground users, leveraging a joint channel prediction and client scheduling algorithm to optimize resource allocation.

Despite these advancements, a scheduling framework that seamlessly integrates path planning with laser charging, jointly optimizes energy and time efficiency, and explicitly addresses uncertainties caused by dynamic meteorological conditions remains an unexplored challenge—one that this paper aims to resolve.

3. Theoretical Framework

In this section, we first formulate the modular vehicle-routing problem (MVRP) for UAVs, and next elucidate the underlying principles of the laser wireless power transmission system (LWPT).

3.1. MVRP Formulation for UAV Scheduling

As a pivotal research direction in intelligent operations research, UAV scheduling technology has demonstrated profound application potential across a variety of industries.

In emergency response and environmental monitoring, real-time UAV scheduling frameworks address time-critical missions such as traffic incident monitoring or disaster relief [1–3]. These models optimize task assignment and flight planning under stringent deadlines and resource constraints, often using multi-objective MILP approaches to maximize coverage, minimize delays, and manage UAV energy consumption. Scheduling systems are designed to tolerate uncertainties in execution (e.g., GPS unreliability, wind disturbance), yielding robust task completion under dynamic conditions.

In intelligent urban logistics hubs, advanced UAV scheduling systems operate as middleware bridging high-level dispatch planning with low-level execution. One "airport–unloading station" architecture supports collaborative scheduling among UAVs and ground personnel to execute urban parcel delivery tasks in real time. Experimental results validate the system's feasibility and its potential for scalable commercial deployment [26].

These applications fundamentally extend the classical MVRP framework. The MVRP is a classic operations research problem that seeks optimal task assignment and path planning for multiple service vehicles. Formally, the problem can be defined as follows: Given a fleet of vehicles and a set of service points, determine the optimal set of routes that minimize total cost while satisfying constraints such as vehicle capacity and service time windows [27]. The MVRP model for UAVs is shown in Figure 1. The dispatch center designs the task path and assigns UAVs to each task point to ensure that tasks are completed in order before reaching the final destination.

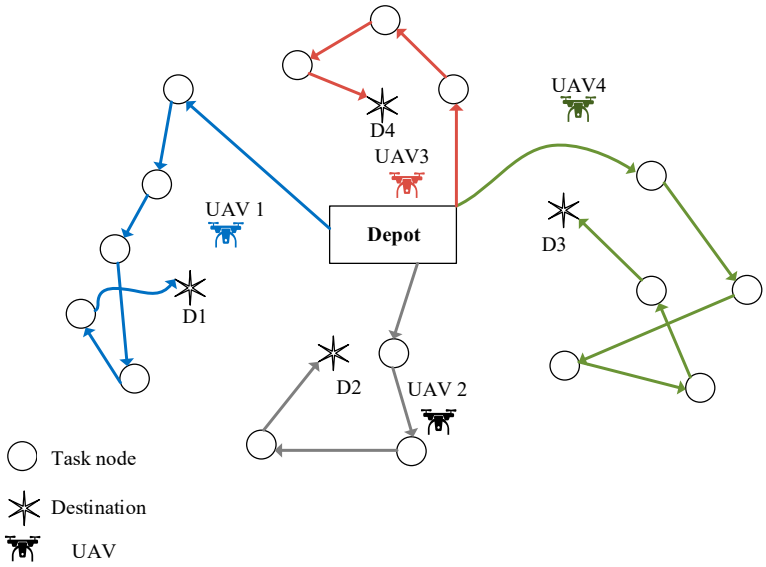


Figure 1. UAV MVRP scheduling modeling diagram.

While traditional MVRP focuses on static constraints like vehicle capacity and time windows, modern UAV scheduling must address additional layers of complexity. For instance, in agricultural applications, the optimal flight path planning for pesticide spraying UAVs must simultaneously account for wind patterns, terrain occlusion, and chemical payload constraints—a multidimensional optimization challenge that conventional MVRP formulations cannot adequately capture.

Our research focuses on a particularly demanding application scenario: post-disaster distribution network recovery. First, a UAV-mounted mobile base station is deployed to the fault location to establish an emergency communication link, thereby restoring the supervisory control and data acquisition (SCADA) connection. Real-time fault detection and isolation are accomplished through data exchange between field devices and the control center. Subsequently, remote operators leverage the emergency communication network to actuate load switches and sectionalizers, enabling partial load restoration. Typically, up to 40% of the load can be recovered before physical repairs commence at the fault site. While this problem shares similarities with conventional MVRP, it presents unique challenges including the spatiotemporal distribution characteristics of power grid faults and the optimal allocation of limited resources. To address these challenges, we propose a novel optimization framework with corresponding solution algorithms, offering innovative technical solutions to improve distribution networks' emergency restoration capacity.

Conventional MVRP methods achieve partial cost reduction but typically decouple UAV charging from mission execution, resulting in substantial operational inefficiencies. To overcome this critical limitation, this study proposes a novel integration of laser charging technology into UAV scheduling. By utilizing non-contact energy transmission, the proposed approach supports simultaneous charging and mission execution, thereby advancing UAV operational optimization. The next section details the operational principles of laser-powered UAV systems.

3.2. The Basic Principles of Laser Charging for UAV

The LWPT system consists of a laser transmitting system and a laser receiving system, as illustrated in Figure 2. The transmitting system includes a power supply, a laser driver, and a transmitting device.

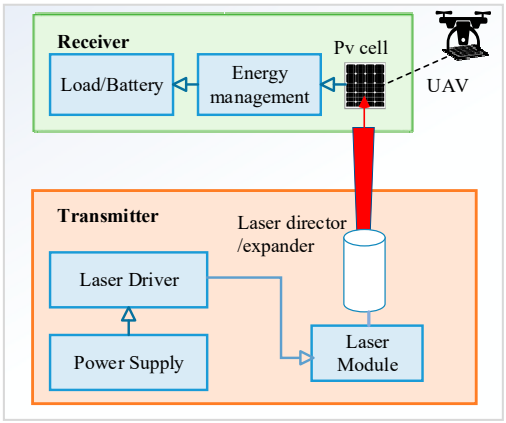


Figure 2. Block diagram of laser wireless power transmission system.

The laser driver and power supply provide stable electrical energy while regulating power and frequency. The laser module converts electrical energy into optical energy, and the transmitting device expands and directs the laser beam. At the receiving end, a photovoltaic (PV) cell mounted on the UAV converts the incident laser back into electrical energy, which is then efficiently managed and stored by the energy management module, ensuring optimal utilization of laser power.

The total efficiency of the LWPT system can be expressed as [28]:

$$\eta = \eta_e \eta_t \eta_r \tag{1}$$

where η is the total transmission efficiency of the system; η_e is the electricity-laser conversion efficiency of the laser; η_t is the transmission efficiency of the laser in the atmosphere; η_r is the laser-electricity conversion efficiency of the receiving device. η_t can be modeled as [29]:

$$\eta_t = e^{-\alpha d} \tag{2}$$

where α is the laser attenuation coefficient, and d is the distance. When d is much less than 1 km, the laser transmission efficiency approaches 100% [30].

In this study, simulations were conducted using an 808 nm laser with an output power of 250 W, with the UAV cluster maintaining a 60 m altitude. η_t was assumed to be 100%, while using a GaAs photovoltaic cell, was assumed to be 50% [31]. Based on the above parameters in this paper the UAV charging power η_t is 125 W.

In recent years, LWPT technology has transitioned from experimental validation to engineering implementation in UAV applications, fundamentally transforming conventional UAV operational paradigms. Early demonstrations include the 2012 collaborative experiment between Laser Motive and Lockheed Martin, where laser-powered long-endurance flight was successfully achieved for the Stalker UAV in wind tunnel conditions [10], enabling continuous operation exceeding 48 h and overcoming traditional battery endurance limitations.

In practical field applications, the laser charging system developed by China Guizhou Power Grid Company has been successfully implemented in 110 kV transmission line inspections. The system demonstrates reliable performance by providing stable wireless power transmission to inspection UAVs within a 300-m operational range, achieving a photoelectric conversion efficiency exceeding 40%. This technological solution effectively enables the "station-based" unmanned inspection paradigm, significantly enhancing intelligent operation and maintenance efficiency for power grid infrastructure [32].

Notably, the University of Washington's RoboFly micro-aircraft demonstrates LWPT's versatility, achieving precise 3-m-range charging. This breakthrough enables novel power solutions for micro-UAV applications including agricultural monitoring and confined-space rescue operations [33].

These advancements collectively demonstrate LWPT's dual impact: significantly enhancing UAV endurance while establishing critical technical foundations for multi-mission coordination, persistent operations, and high-frequency scheduling strategies in unmanned aircraft systems.

4. System Model

The increase in extreme natural disasters exposes distribution networks to complex scenarios involving simultaneous power outages and communication failures, posing significant challenges to post-disaster recovery. Restoring power communication systems is critical to enabling distribution network recovery, particularly in distribution automation based restoration strategies.

This paper proposes a cooperative UAV cluster-based load recovery model, where UAVs serve as emergency communication base stations to restore connectivity to fault-affected nodes. Once communication is reestablished, these nodes can receive remote control commands from the dispatch center, facilitating rapid load recovery. The proposed model is formulated under the following assumptions:

1. UAV Operation Constraints: The UAV cluster departs from the dispatch center, visits designated work points, and returns to the dispatch center. Each UAV has identical energy capacity and experiences uniform path loss during flight.
2. Energy Consumption Model: The energy consumption of UAVs is dominated by hovering and mobility, while communication energy costs are negligible.
3. Fault Point Handling: The coordinates of fault points are assumed known, and UAVs are equipped with laser-based charging systems to replenish their energy when servicing fault points.
4. Charging rules: The charging protocol initiates upon arrival at the designated task point, where laser charging systems distribute energy evenly across all UAVs in the cluster to maintain approximate state-of-charge parity among units.

The laser-powered UAV-assisted load recovery model is illustrated in Figure 3. Following a disaster, the scheduling center obtains fault point information and dispatches an appropriate number of UAVs to form clusters. Each cluster is assigned a task path. The UAV clusters depart from the dispatching center, restore communication at designated task nodes along their paths, and return upon task completion. At task points, the UAVs can recharge via ground-based laser power transmission.

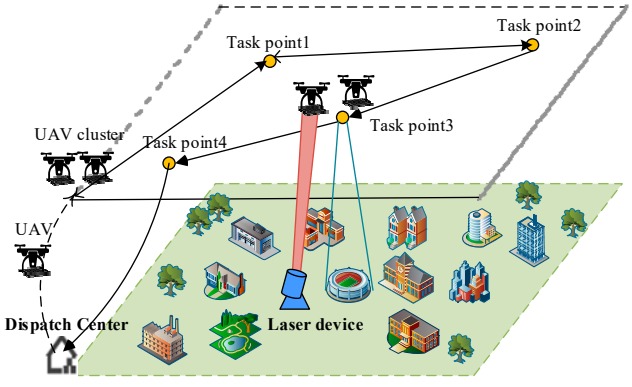


Figure 3. Laser UAV-assisted load recovery model.

4.1. Laser UAV Model

We establish a two-dimensional cartesian coordinate system with the dispatch center positioned at the origin (0,0). Following a disaster-induced distribution network fault, the dispatch center acquires the geographical coordinates of the target work point requiring communication restoration. Subsequently, it computes the optimal task path for the UAV cluster. The cluster then executes the dispatched task by navigating to the designated work point and ultimately returning to the dispatch center upon task completion. We define the set of UAV tasks as $\theta = \{\theta_1, \theta_2 \ldots, \theta_n\}$, where θ_1 and θ_n represent the starting and ending points of the task, respectively, and both are coordinate systems of the scheduling center, using a binary indicator function $x_{i,j,u} \in \{0,1\}$ to represent the task selection variable. The binary variable indicates whether UAV cluster u traverses from task node i to task node j. Table 1 lists the principal symbols employed throughout this paper.

Table 1. List of major notations.

Symbol	Notations
$\theta = \{\theta_1, \theta_2 \ldots, \theta_n\}$	Fault points (task points) and dispatch centers set data
U = {1,2,3. . .u}	Numbered sets of UAV clusters
N	Total number of UAVs
P_{ch}	Laser charging power
e_{ij}	Power consumption for passage between nodes i, j
E_u^{max}	Battery capacity of UAV cluster u
$x_{i,j,u}$	Task selection variable
n_u	Number of UAVs in UAV cluster u
$E_{i,u}^{after}$	Electricity of UAV cluster u when leaving node i
$E_{i,u}^{before}$	Electricity of UAV cluster u when reaching node i
$t_{i,u}^{task'}$	The task time for UAV cluster u at node i
t_i^{task}	The task time for single UAV at node i
$t_{i,j}$	The time it takes for the UAV to fly from node i to node j
$t_{i,u}^{char}$	The charging time of UAV cluster u at node i UAV
$t_{i,u}^{park}$	The dwell time of UAV cluster u at node i
P_h	Hovering power
P_f	Flight power consumption
$\widetilde{\theta}$	Set of critical points to be recovered
W_i	Node i communication recovery status
ρ_i	Conforming load recovery after node i is communication resumption
T_a	Task scheduling limit time

In our work, we assume that there are multiple UAV clusters working, and the routing and capacity constraints of the UAV cluster scheduling model are as follows:

$$0 \le n_u \le N, \sum_{\forall u \in U} n_u \le N \tag{3}$$

$$\sum_{\forall i \in \theta} x_{i,j,u} - \sum_{\forall k \in \theta} x_{j,k,u} = 0, \ \ \forall j \in \theta, j \notin \{\theta_1, \theta_n\}, \forall u \in U \tag{4}$$

$$\sum_{\forall i \in \theta} x_{i,j,u} = 0, \sum_{\forall k \notin \theta} x_{j,k,u} = 1, \ \ \forall j \in \{\theta_1\}, u \in U \tag{5}$$

$$\sum_{\forall i \in \theta} x_{i,j,u} = 1, \sum_{\forall i \in \theta} x_{i,j,u} = 0, \ \ \forall j \in \{\theta_n\}, u \in U \tag{6}$$

$$\sum_{\forall i \in \theta} x_{i,j,u} + \sum_{\forall j \in \theta} x_{j,i,u} \leq 1, \ \ \forall u \in U \tag{7}$$

$$0 \leq E_{i,u}^{\text{before}} \leq E_u^{\max}, \ 0 \leq E_{i,u}^{\text{after}} \leq E_u^{\max}, \ \ \forall i \in \theta, u \in U \tag{8}$$

$$n_{\text{u}} \geq 0, \ \ \forall u \in U \tag{9}$$

$$\sum_{\forall i} x_{i,i,u} = 0, \ \ \forall u \in U \tag{10}$$

$$-(1 - x_{i,j,u})M \leq E_{i,u}^{\text{after}} - e_{ij} - E_{j,u}^{\text{before}} \leq (1 - x_{i,j,u})M, \ \ \forall i, j \in \theta, \forall u \in U \tag{11}$$

$$\sum_{i \in \theta} \sum_{u \in U} x_{i,j,u} \leq 1, \sum_{i \in \theta} \sum_{u \in U} x_{i,z,u} = 1, \ \ \forall j \in \theta, \ j \notin \{\theta_1, \theta_n\}, \ z \in \widetilde{\theta}, \widetilde{\theta} \subseteq \theta \tag{12}$$

$$x_{i,j,u} \in \{0, 1\}, \ \ \forall i, j \in \theta, u \in U \tag{13}$$

$$W_i = \sum_{j \in \theta} \sum_{u \in U} x_{j,i,u}, \ \ \forall i \in \theta, \ i \notin \{\theta_1, \theta_n\} \tag{14}$$

$$e_{ij} = t_{ij} \cdot P_f, \ \ \forall i, j \in \theta \tag{15}$$

Constraint (3) limits that the sum of the number of UAVs in all UAV clusters cannot exceed the total number of UAV clusters that can be dispatched by the dispatch centre. Constraint (4) ensures the continuity of the mission path, i.e., the UAVs follow the mission path to the next mission point after executing the current mission. Constraints (5) and (6) ensure that UAV clusters can only fly out from the initial point to fly back to the end point after executing the path according to the mission path planned by the dispatch centre. Constraints (7) and (10) ensure that the mission path follows a unidirectional non-round-trip rule, hence the need to add the elimination loop constraint. Constraint (8) indicates that the UAV cluster u maintains its power within the normal range during the work at work point i. Constraint (9) is a non-negative condition for n_p, and it is an integer variable. Constraint (11) represents the power state of the UAV cluster when it reaches work point j, where M is a slack variable, and $E_{i,p}^{after}$ denotes the power level when the UAVs leave work point i. $E_{j,p}^{before}$ denotes the variable when the UAV reaches workpoint j. Constraint (12) ensures that every task node at most has a cluster of UAVs working on it, considering the actual situation of load restoration of the distribution network, the primary restoration is realized for the key task nodes, and the secondary task nodes are restored according to the actual situation. Constraint (13) is a task path selection variable whose value of 1 indicates that UAV cluster p traverses from task node to task node. Constraint (14) establishes the coupling relationship between task path selection variables $x_{i,j,u}$ and the communication restoration state of faulted nodes, where $W_i \in$ {0,1} denotes the recovery status of node i. Constraint (15) models the UAV's energy consumption during flight between task points.

Considering the range of the UAV, we use laser charging technology to charge the UAV. With this technology the UAV can be charged at a distance and can work normally at the hovering work point while charging. Considering laser charging, there are the following constraints:

$$E_{i,u}^{after} = E_{i,u}^{\text{before}} + t_{i,u}^{\text{char}} P_{ch} - t_{i,u}^{\text{park}} P_h, \ \ \forall i, j \in \theta, \forall u \in U \tag{16}$$

$$t_{i,\text{u}}^{\text{park}} = \max\left\{ t_{i,u}^{\text{task}'}, t_{i,u}^{\text{char}} \right\} \ \ \forall i \in \theta, \forall u \in U \tag{17}$$

$$t_{i,u}^{\text{task}'} = \begin{cases} t_i^{task}/n_u, n_u > 0 \\ 0, n_u = 0 \end{cases}, \ \ \forall i \in \theta, \forall u \in U \tag{18}$$

$$\sum_{i,j\in\theta}(t_{ij}+t_{j,u}^{park})x_{i,j,u}\le T_a,\ \ \forall u\in U \tag{19}$$

Constraint (16) defines the energy dynamics of UAV cluster u upon departure from a laser-equipped task site, where the departure energy is computed as the sum of the arrival energy and the energy replenished via laser charging, minus the energy expended during hovering operations. Constraint (17) specifies the residence time of the UAV cluster u at mission node i, defined as the maximum between the charging duration and the task execution time of the cluster. Constraint (18) relates the task execution time of UAV cluster u at node i to the number of UAVs in the cluster. Constraint (19) ensures that the total time taken by each UAV cluster to complete all assigned missions does not exceed the overall mission scheduling time.

The model's objective function is formulated to maximize the total restored load at the failed node.

$$\begin{aligned} Max\quad & \sum_{i=2}^{f-1} W_i\rho_i \\ & s.t\ (3)\text{–}(19) \end{aligned} \tag{20}$$

This model is formulated as a mixed-integer programming (MIP) problem. Apart from Constraints (17)–(19), the entire model remains linear. The nonlinear constraints can be effectively linearized, thereby transforming the problem into a mixed-integer linear programming (MILP) formulation, which can be efficiently solved using commercial optimization solvers.

The maximization operation in Constraint (17) is linearized via binary variables, employing a well-established technique documented in classical optimization literature [34]. We employ two binary decision variables, a and b, to transform the nonlinear maximization operation into an equivalent mixed-integer linear formulation as follows:

$$\begin{cases} t_{i,u}^{\text{park}}\ge t_{i,u}^{\text{task}'}, t_{i,u}^{\text{park}}\ge t_{i,u}^{\text{char}} \\ t_{i,u}^{\text{park}}\le t_{i,u}^{\text{task}'}+M(1-a) \\ t_{i,u}^{\text{park}}\le t_{i,u}^{char}+M(1-b) \\ a+b=1,\ a,b\in\{0,1\} \end{cases},\ \forall i\in\theta,u\in U \tag{21}$$

where M is a predetermined large constant (M = 10^3 in our implementation). Following the piecewise linearization technique in [35], we handle constraint (18) by dividing the interval [1,N] into K segments with breakpoints $1 = d_0 < d_1 < \ldots < d_K = \text{N}$ and introduce the binary variable δk to select the interval segments for n_u:

$$\begin{cases} \sum_{k=1}^{K}\delta_k\le 1 \\ n_u\ge d_{k-1}-(1-\delta_k)M \\ n_u\le d_k+(1-\delta_k)M \end{cases},\ \forall k\in\{1,\ldots,K\},u\in U \tag{22}$$

By performing a first-order Taylor linear expansion at the midpoint mk of each zone, Constraint (18) can be transformed into:

$$t_{i,u}^{\text{task}\prime}=t_i^{task}\sum_{\text{k}=1}^{K}\delta_k\left(\frac{1}{m_k}-\frac{1}{m_k^2}(n_u-m_k)\right),\forall i\in\theta,u\in U \tag{23}$$

For Constraint (19), we introduce the auxiliary variable $y_{i,j,u} = t_{j,u}^{park} \cdot x_{i,j,u}$, then we have the following constraints:

$$\begin{cases} y_{i,j,u} \le M \cdot x_{i,j,u} \\ y_{i,j,u} \le t_{j,u}^{park} \\ y_{i,j,u} \ge t_{j,u}^{park} - M \cdot \left(1 - x_{i,j,u}\right) \\ y_{i,j,u} \ge 0 \end{cases}, \forall i, j \in \theta, \forall u \in U \tag{24}$$

Similarly, Constraint (19) consists of continuous $t_{j,u}^{park}$ multiple binary variable $x_{i,j,u}$, which can be transformed into the following:

$$\sum_{i,j \in \theta} \left(t_{\mathrm{ij}} \cdot x_{i,j,u} + y_{i,j,u}\right) \le T_a, \quad \forall u \in U \tag{25}$$

After the linearization process, the proposed model can be reformulated as:

$$\begin{aligned} &Max \sum_{i=2}^{\mathrm{n}-1} W_i \rho_i \\ &s.t\ (3)\text{–}(16),\ (21)\text{–}(25) \end{aligned} \tag{26}$$

4.2. DRO Model Formulation

The operational performance of UAVs, including energy consumption patterns, flight velocity, and trajectory stability, exhibits significant variability under adverse meteorological conditions (e.g., high winds, precipitation, and snowfall). These environmental factors collectively contribute to substantial uncertainties in the estimated time of arrival (ETA), as illustrated in Figure 4. To robustly address this uncertainty, we propose a DRO framework incorporating distributed ambiguous chance constraints. The methodology explicitly characterizes flight time uncertainty through a carefully constructed Gaussian perturbation ambiguity set, following the modeling approach referenced in prior work. Furthermore, we develop a computationally tractable safe convex approximation that reformulates the original DRO problem as a mixed-integer second-order cone program (MISOCP), while preserving the solution robustness.

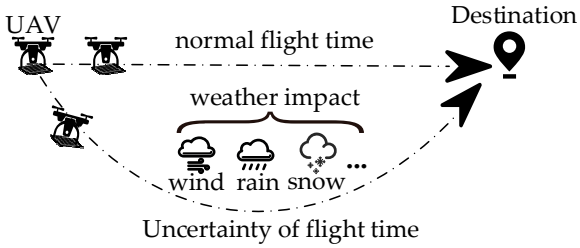


Figure 4. Effect of weather on UAV flight time.

We model the uncertain flight time between task points as: $t_{ij} = \overline{t_{ij}} + \xi_{ij} \cdot \hat{t_{ij}}, \forall i, j \in \theta$, where $\overline{t_{ij}}$ is the normal flight time between node i and j, calculated by dividing the distance between task points by the average flight speed of the UAV. $\hat{t_{ij}}$ is the deviation of the uncertain flight time, and ξ_{ij} represents a random perturbation variable with partial probability distribution information. Given a general ambiguous set, we first introduce the ambiguous chance constraint of constraint (24) as follows:

$$\inf_{p \in P} \mathrm{Prob}_{\xi \sim P} \left\{ \sum_{j \in \theta} \overline{\Delta}_{ij} + \sum_{j \in \theta} y_{i,j,u} + \sum_{j \in \theta} \xi_{ij} \cdot \hat{\Delta}_{ij} \le T_a \right\} \ge 1 - \epsilon,\ \forall i \in \theta, u \in U \tag{27}$$

In (27), $\overline{\Delta}_{ij} = \overline{t}_{ij} x_{i,j,u}$, $\hat{\Delta}_{ij} = \hat{t_{ij}} x_{i,j,u}$, $\epsilon \in (0,1)$ indicates confidence level, $\inf_{p \in \mathcal{P}}\{\cdot\}$ is used to denote the worst-case scenario, i.e., robustness. Using $\text{Prob}_{\tilde{\xi} \sim P}(\cdot)$ to denote the probability of the time under the probability distribution, where only partial statistical information—namely, the mean and variance—is known a priori. Based on the model developed in the previous section, the following DRO model is proposed:

$$\begin{aligned} &[initital\ DRO]\ Max \sum_{i=2}^{n-1} W_i \rho_i \\ &s.t.\ Constra\text{ints } (3)\text{–}(15),\ (21)\text{–}(25),\ (27) \end{aligned} \tag{28}$$

The proposed DRO model is a semi-infinite programming problem, which is computationally difficult to handle for general inexact sets. So in this section, we design an inexact set that may be obeyed by uncertain flight times, the Gaussian set P_1.

$$P_1 = \left\{ P : E_P[\xi_{ij}] = [\mu_{ij}^-, \mu_{ij}^+],\ V_P[\xi_{ij}] \le \sigma_{ij}^2,\ \forall i, j \in \theta \right\} \tag{29}$$

where E_P and V_P denote the mean and variance of the random variable respectively, We use u_{ij}, s_{ij}^2 to denote the E_P and V_p, thus have $u_{ij} \in [\mu_{ij}^-, \mu_{ij}^+]$, $s_{ij}^2 \le \sigma_{ij}^2$. Based on the standard normal distribution, the chance constraint (27) is normalized and the following results are obtained:

$$\inf_{P \in \mathcal{P}} \text{Prob}_{\tilde{\xi} \sim P} \left\{ \frac{\sum_{i,j \in \theta} (\xi_{ij} - \mu_{ij}) \hat{\Delta}_{ij}}{\sqrt{\sum_{i,j \in \theta} (s_{ij} \cdot \hat{\Delta}_{ij})^2}} \le \frac{T_a - \sum_{i,j \in \theta} (\overline{\Delta}_{ij} + \mu_{ij} \cdot \hat{\Delta} t_{ij} + y_{i,j,u})}{\sqrt{\sum_{i,j \in \theta} (s_{ij} \cdot \hat{\Delta}_{ij})^2}} \right\} \ge 1 - \epsilon,\ \forall u \in U \tag{30}$$

According to the distribution function of the standard normal distribution $\Phi(x) = \text{P}\{X \le x\}$, $X \sim \text{N}(0,1)$, it can be obtained:

$$\Phi \left(\frac{T_a - \sum_{j \in \theta} (\overline{\Delta}_{ij} + \mu_{ij} \cdot \hat{\Delta}_{ij} + y_{i,j,u})}{\sqrt{\sum_{j \in \theta} (s_{ij} \cdot \hat{\Delta}_{ij})^2}} \right) \ge 1 - \epsilon,\ \forall i \in \theta \tag{31}$$

Utilizing the monotonicity of $\Phi(\cdot)$, we apply the inverse standard normal cumulative distribution function $\Phi^{-1}(\cdot)$ to both sides:

$$\frac{T_a - \sum_{j \in \theta} (\overline{\Delta}_{ij} + \mu_{ij} \cdot \hat{\Delta}_{ij} + y_{i,j,u})}{\sqrt{\sum_{j \in \theta} (s_{ij} \cdot \hat{\Delta}_{ij})^2}} \ge \Phi^{-1}(1 - \epsilon),\ \forall i \in \theta \tag{32}$$

When $\epsilon < 1/2$, $\Phi^{-1}(1 - \epsilon) > 0$. By rearranging, the formula (32) can be rewritten as:

$$\sum_{i.j \in \theta} (\overline{\Delta}_{ij} + \mu_{ij} \cdot \hat{\Delta}_{ij} + y_{i,j,u}) + \Phi^{-1}(1 - \epsilon) \sqrt{\sum_{i,j \in \theta} (s_{ij} \cdot \hat{\Delta}_{ij})^2} \le T_a,\ \forall u \in U \tag{33}$$

To ensure robustness, we consider the worst-case scenario with maximum time-of-flight perturbation, as follows:

$$\max \left\{ \sum_{i,j \in \theta} (\overline{\Delta}_{ij} + \mu_{ij} \cdot \hat{\Delta}_{ij} + y_{i,j,u}) + \Phi^{-1}(1 - \epsilon) \sqrt{\sum_{i,j \in \theta} (s_{ij} \cdot \hat{\Delta}_{ij})^2} \right\} \le T_a,\ \forall u \in U \tag{34}$$

Given the uncertainty intervals $u_{ij} \in [\mu_{ij}^-, \mu_{ij}^+]$ and $s_{ij}^2 \leq \sigma_{ij}^2$, the preceding formulation can be further simplified as follows:

$$\sum_{i,j\in\theta} \overline{\Delta}_{ij} + \sum_{i,j\in\theta} \max\left[\mu_{ij}^- \cdot \hat{\Delta}_{ij}, \mu_{ij}^+ \cdot \hat{\Delta}_{ij}\right] + \Phi^{-1}(1-\epsilon) \cdot \sqrt{\sum_{i,j\in\theta} (\sigma_{ij} \cdot \hat{\Delta}_{ij})^2} + \sum_{i,j\in\theta, u\in U} y_{i,j,u} \leq T_a \quad (35)$$

Based on the above theory, and considering flight time uncertainty, we propose the equivalent formulation of the tractable DRO model under ambiguous $\mathcal{P}_1$ set as follows:

$$\begin{aligned} &[solvable\ DRO]\ Max \sum_{i=2}^{n-1} W_i \rho_i \\ &s.t.\ Constra\text{ints } (3)\text{–}(15),\ (21)\text{–}(25),\ (36) \end{aligned} \quad (36)$$

The proposed model is a MISOCP, characterized by integer decision variables $x_{i,j,u}$ and a second-order cone constraint involving the term $\sqrt{\sum_{i,j\in\theta} (\sigma_{ij} \cdot \hat{\Delta}_{ij})^2}$ in (34). This class of models can be efficiently solved using commercial solvers (e.g., Gurobi, CPLEX).

5. Simulation Results

5.1. Simulation Setup

The simulations in this study were performed on a computational system equipped with a 3.00 GHz processor, 32 GB of RAM, and a 64-bit operating system. The optimization model was implemented and solved in Gurobi 12.0, with the mixed-integer programming (MIP) tolerance configured as MIPGap = 20%. The key parameters used in the UAV simulation are summarized in Table 2. Core performance metrics—including battery capacity, hovering power, and flight power consumption—are derived from specifications of the DJI Air 3S UAV. Parameters related to laser charging, such as the 125 W power input, are set according to experimentally reported photoelectric conversion efficiencies and system loss characteristics [30,31]. Together with task-informed scheduling durations, these parameter choices are intended to support the practical relevance and validity of the simulation results.

Table 2. UAV related parameters.

Parameter	Value
Battery capacity	4276 mAh
Hovering power consumption	90 W
Flight power consumption	80 W
Laser charging power	125 W
Total number of UAVs	100
Flight speed	15 m/s
Number of UAV clusters	6
Nominal battery voltage	14.6 V
Battery energy	62.5 Wh
Task scheduling limit time	60 min

In this section, the proposed multi-UAV cluster cooperative distribution network load recovery model is validated through an example. Assuming that the coordinates of the fault point are known, the UAV dispatch center is located at the origin, and there are laser devices around each fault point to charge the UAVs, the UAVs assist in load restoration by restoring the communication for the fault point. As shown in Figure 5, nodes 2–20 are the coordinates of the fault points. We assume that the recoverable load per faulty node via UAV aid is given. Figure 6 displays the preset load recovery values, the corresponding

load recovery for node 15 after restoring communications is 0.4. The design and analysis of results for multiple sets of arithmetic cases are presented separately below.

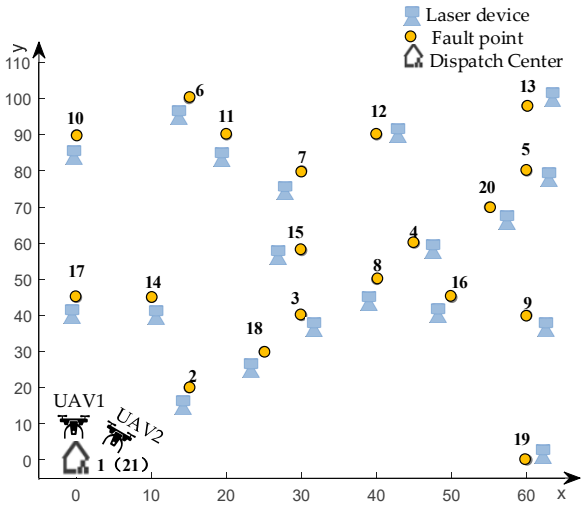


Figure 5. Fault point coordinate diagram. Note: All distance values in this figure represent actual meters divided by a scale factor of 150.

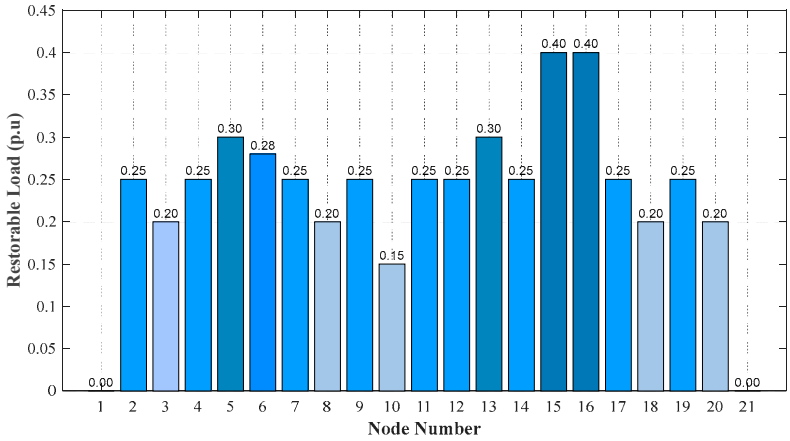


Figure 6. Estimated node load recovery.

The task completion time required by a single UAV to service each individual faulty node is assumed to be known a priori. As shown in Figure 7, the mission duration of a single UAV at node 9 is 50 min.

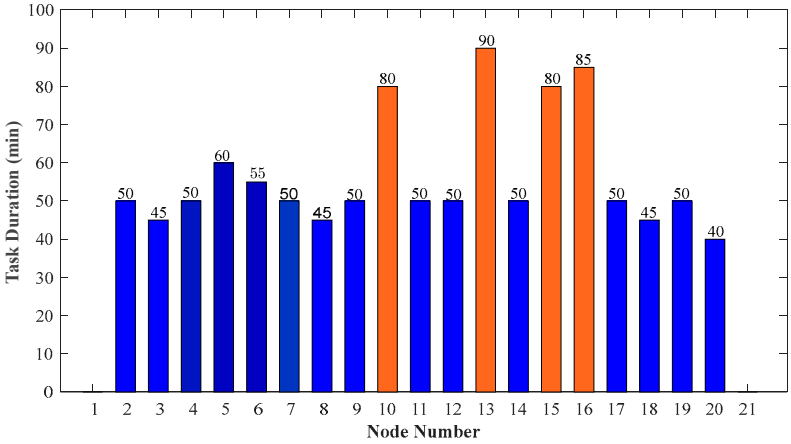


Figure 7. Task completion time per node for single UAV operation.

5.2. Comparative Analysis of Scheduling Strategies

In this section, a set of comparative experiments is conducted to evaluate the effectiveness of the proposed model. The experimental setup is defined as follows: based on the urgency of power load restoration, nodes 2, 3, 15, and 18 are designated as critical load nodes, denoted by the set $\widetilde{\theta} = \{\theta_2, \theta_3, \theta_{15}, \theta_{18}\}$, while the remaining nodes are considered secondary. The scheduling objective is to maximize load recovery by prioritizing the restoration of critical loads within a given time frame and selectively recovering secondary nodes under residual resource constraints. Building upon the conventional MVRP scheduling model, four comparative scenarios are constructed by incrementally incorporating UAV energy limitations, laser charging constraints, and flight robustness requirements.

1. Baseline model: traditional MVRP scheduling without considering any UAV operational constraints.
2. Energy constraint modeling: adding UAV energy constraints to the baseline model.
3. Charging extension model: adding laser charging to the range constraint model
4. Robust optimization model: introducing flight robustness constraints based on the charging extension model. Considering the uncertain parameters, we set $\hat{\Delta}t_{ij} = 0.1 \cdot \overline{\Delta}t_{ij}$ for DRO model. In particular, u_{ij}^{+}, u_{ij}^{-} are randomly generated from $[-1, 1]$, and σ_{ij} are randomly generated from $[0, 0.1]$, $\forall i, j \in \theta$, $\epsilon = 0.1$.

Notably, the UAV cluster prioritizes auxiliary power restoration for critical load nodes when resource conflicts occur. Table 3 describes the UAV cluster dispatches and load recovery in the four cases, and Figures 8–11 illustrate the task path diagrams of UAV clusters in different cases.

Table 3. Number of UAVs in cluster.

U	Case1		Case2		Case3		Case4	
	n_u	ρ/p.u	n_u	ρ/p.u	n_u	ρ/p.u	n_u	ρ/p.u
1	15	0.93	23	0.75	45	1.3	32	0.75
2	0	0	22	1.15	13	0.85	21	0.55
3	40	1.05	15	0.45	15	0.35	15	0.9
4	23	1.15	21	0.6	18	1.3	21	1.05
5	15	1.0	10	0.5	5	0.28	9	0.53
6	7	0.75	9	0.25	4	0.5	2	0.25
Total	100	4.88	100	3.60	100	4.58	100	4.03

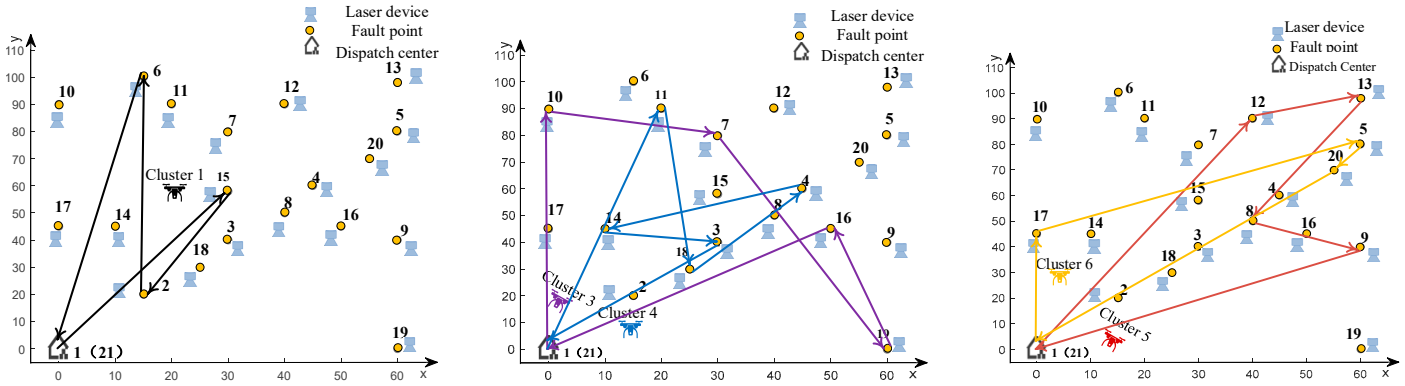


Figure 8. Cluster task path diagram in case 1.

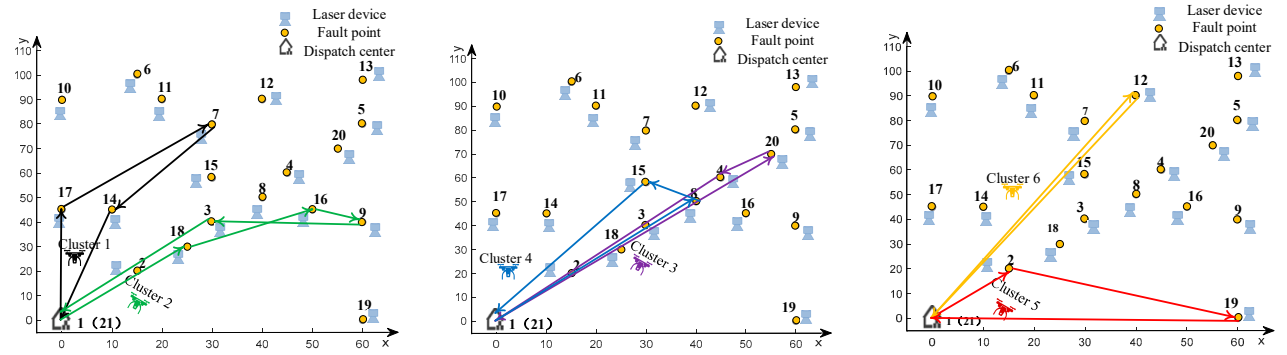


Figure 9. Cluster task path diagram in case 2.

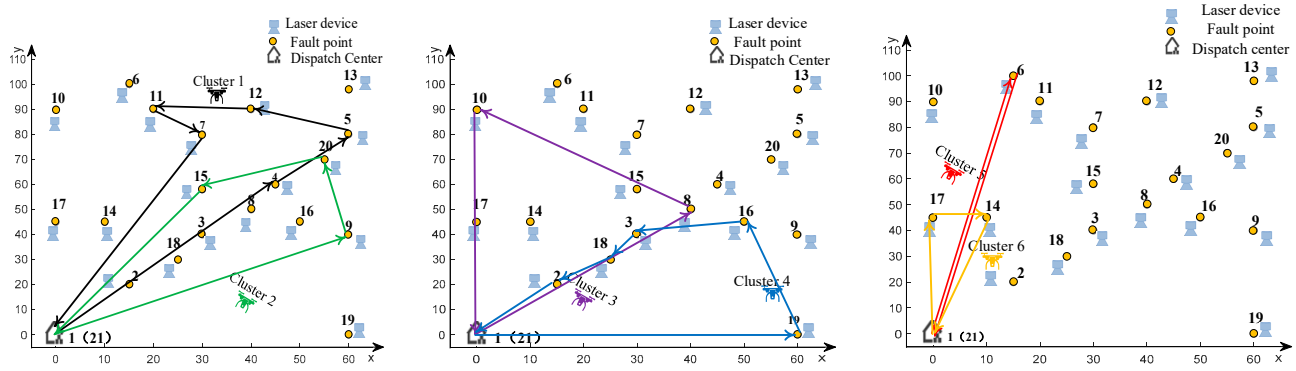


Figure 10. Cluster task path diagram in case 3.

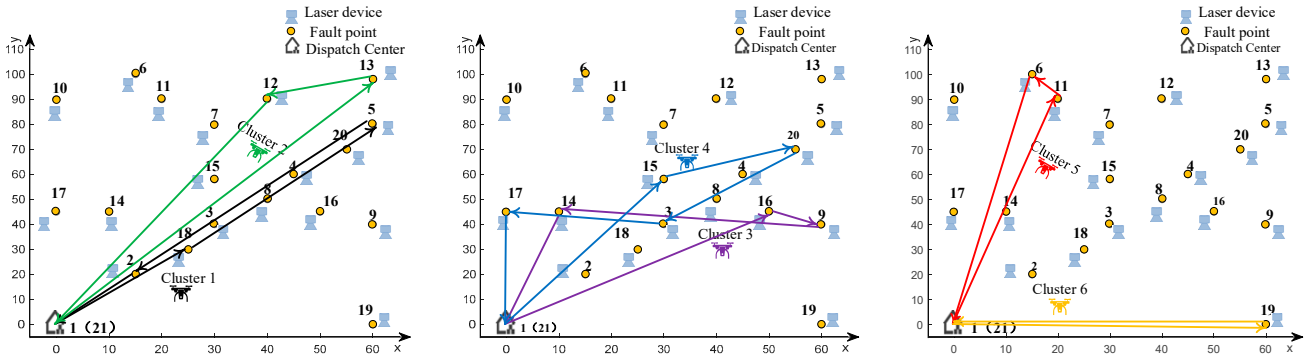


Figure 11. Cluster task path diagram in case 4.

From the data in Table 2, it can be noted that the total amount of load recovered by UAV cluster assisted recovery is the largest for the ideal case without energy consumption in case 1, and the total amount of load recovered by UAV cluster assisted recovery is the smallest for case 2, which only considers energy consumption without charging. Due to the lack of range supplementation, the total amount of load recovered by the UAVs in case 2 is still undesirable even though all of them are dispatched to perform the task, and for this reason the laser charging mechanism is introduced. Charge the UAVs during the task execution at the task point until the remaining power of the UAVs is sufficient to reach the next task point after the task is completed. The load recovery in the simulation of case 3 is only slightly lower than the load recovery in case 1. The amount of load recovery in the simulation of case 4, which takes into account the flight time uncertainty, is lower than that in case 3. This is mainly due to the uncertainty of the flight time and the laser charging time, as the system adopts a safer and more conservative scheduling strategy with a relatively lower load recovery during the limited task time. Despite this, Table 2 shows that the total

amount of load recovery of our proposed DRO model is much higher than that of case 2, and the proposed model is effective.

From Figures 8–11 UAV path planning graphs for different cases, it can be observed that case 1 ideally has the highest number of nodes visited by UAVs, case 2 has the smallest number of nodes visited by UAVs considering energy consumption, and the number of accessed nodes in cases 3 and 4 shows a slight decrease compared to case 1. Critical load restoration nodes set up in different scenarios have all been visited.

5.3. Sensitivity Analysis

Our analysis investigates the impact of confidence interval variations and task scheduling durations (40, 50, 60, and 70 min) on the optimal solutions of the DRO model. All other parameters remain consistent with the settings described in the preceding section, ensuring a controlled comparative evaluation.

As evidenced by Table 4, the total load recovery exhibits a positive correlation with task scheduling duration. Under identical durations, however, recovery capacity declines with expanding confidence intervals. This inverse relationship stems from the trade-off between tolerance for uncertainty flight time and operational conservatism: wider confidence intervals enforce stricter robustness margins, necessitating reduced load restoration to maintain probabilistic feasibility. Notably, at Ta = 50, identical recovery values for 75% and 80% confidence intervals suggest potential suboptimal convergence due to the MIPGap = 20% termination threshold.

Table 4. DRO optimization results for different task durations and confidence levels.

Ta/min	Confidence Interval	Total Load Restored/p.u
40	75%	3.65
	80%	3.60
	85%	3.38
	90%	3.20
	95%	3.00
50	75%	4.18
	80%	4.18
	85%	4.08
	90%	3.98
	95%	3.83
60	75%	4.48
	80%	4.34
	85%	4.25
	90%	4.03
	95%	3.93
80	75%	4.73
	80%	4.58
	85%	4.30
	90%	4.18
	95%	3.98

5.4. Computational Efficiency

To assess the computational efficiency of the proposed DRO model, we conducted simulations across varying numbers of faulty nodes while maintaining a fixed UAV cluster size. The node coordinates were randomly generated within a 100 × 100 Cartesian system, with the scheduling center positioned at (0, 0). Critical nodes were defined as four randomly selected fault-affected nodes. The task duration was constrained to 50 min, and the load

recovery value for each node is randomly selected from the interval [0, 0.4]. All other simulation parameters aligned with the configurations described in the preceding section.

Table 5 presents a comparison of the optimization results for different numbers of nodes, highlighting three key metrics: MIPGap, the objective function value, and computation time. As the MIPGap value decreases, the computation time exhibits a notable increasing trend. When the MIPGap reduces from 40% to 20%, the increase in the objective function value is relatively limited. For example, from 4.94 to 5.08 in the 30-node case, representing an approximate 2.8% increase. Considering the significant increase in computation time as the MIPGap decreases, selecting a MIPGap value of 30% in practical applications offers a favorable trade-off between solution accuracy and computational efficiency. As the number of faulty nodes increases, the solution time becomes particularly large when the MIPGap is small, due to the limited number of UAVs in the model. In such cases, it becomes challenging to support practical applications. Therefore, it may be advisable to either terminate the solution process earlier or consider alternative solution methods, such as heuristic optimization algorithms.

Table 5. Optimization results for different node counts.

Nodes	MIP Gap	Objective Functions	Computation Time/s
15	60%	2.4	53
	40%	2.85	94
	30%	2.9	101
	20%	3.13	107
20	60%	3.08	1047
	40%	3.78	1125
	30%	3.89	1578
	20%	4.05	1726
25	60%	4.42	1225
	40%	4.94	1576
	30%	5.03	2063
	20%	5.08	2454
30	60%	5.07	1084
	40%	5.49	1551
	30%	5.70	2883
	20%	/	>4500

6. Conclusions and Outlook

In this paper, we propose a multi-UAV cluster-based assisted load restoration model for the post-disaster load restoration problem of distribution networks. Firstly, considering the UAV battery capacity limitation and flight path time cost, a laser charging mechanism is introduced based on the traditional MVRP model to establish a laser UAV-assisted load restoration model. Second, considering the uncertainty of flight time in actual task execution, a distributed robust chance-constrained planning method is proposed to maximize the total amount of node load recovery on the fuzzy set. We derive a safe and easy-to-handle approximation form under the Gaussian fuzzy set, and obtain a MISOCP model that can be solved by a commercial solver. Finally, through comprehensive simulation experiments, we compared the load recovery performance of different scheduling algorithms under four distinct cases. Additionally, we systematically assess the sensitivity and computational speed.

Future work will focus on advancing the proposed framework in both algorithmic refinement and practical implementation. Key directions include the development of high-fidelity energy consumption models incorporating aerodynamic nonlinearities and

environmental factors, along with extending the scheduling strategy to heterogeneous UAV fleets with diverse operational and energy characteristics. We also plan to integrate robust communication architectures and fault-tolerant mechanisms to enhance system resilience under real-world disruptions.

Furthermore, this research will be extended to develop more comprehensive grid restoration models that incorporate complex practical constraints, including economic-emergency trade-offs and intelligent collaborative decision-making. Advanced optimization algorithms will be explored to improve computational efficiency and scalability for large-scale power systems. To address extreme uncertainty and scalability limitations, we intend to develop hierarchical optimization structures and adaptive learning mechanisms. The integration of real-time data assimilation and digital twin technologies will be investigated to improve system responsiveness and adaptability in dynamic disaster environments. Additionally, adaptive laser charging protocols that comply with safety regulations and dynamic operational constraints will be designed, with experimental validation through field trials and industry collaboration to evaluate performance under realistic disaster response scenarios.

Author Contributions: Conceptualization, X.H. and Y.Z.; Software, X.H. and H.L.; Validation, X.H. and H.L.; Investigation, X.H.; Data curation, X.H.; Supervision, Y.Z. All authors have read and agreed to the published version of the manuscript.

Funding: This research was funded by National Natural Science Foundation of China, U22B2095.

Data Availability Statement: Data are contained within the article.

Conflicts of Interest: The authors declare no conflicts of interest.

References

1. Hao, Z.; Yu, H.; Yu, W.; Binbin, L.; Yi, C.; Cong, W.; Ning, Z. Design and Implementation of UAV Inspection and Control Platform for Transmission Lines. In Proceedings of the 2023 8th International Conference on Information Systems Engineering (ICISE), Dalian, China, 23–25 June 2023.
2. Wang, R.; Wu, W.; Fu, Z.; Chen, B.; Wu, X. Task Scheduling Optimization for UAV Electrical Image Fault Detection with Wireless Power Transfer. *J. Circuits Syst. Comput.* **2024**, *33*, 2450213. [CrossRef]
3. Ojetunde, B.; Ano, S.; Sakano, T. A Practical Approach to Deploying a Drone-Based Message Ferry in a Disaster Situation. *Appl. Sci.* **2022**, *12*, 6547. [CrossRef]
4. Huang, H.; Savkin, A.V. Deployment of Charging Stations for Drone Delivery Assisted by Public Transportation Vehicles. *IEEE Trans. Intell. Transp. Syst.* **2022**, *23*, 15043–15054. [CrossRef]
5. Townsend, A.; Jiya, I.N.; Martinson, C.; Bessarabov, D.; Gouws, R. A Comprehensive Review of Energy Sources for Unmanned Aerial Vehicles, Their Shortfalls and Opportunities for Improvements. *Heliyon* **2020**, *6*, e05285. [CrossRef]
6. Chittoor, P.K.; Chokkalingam, B.; Mihet-Popa, L. A Review on UAV Wireless Charging: Fundamentals, Applications, Charging Techniques and Standards. *IEEE Access* **2021**, *9*, 69235–69266. [CrossRef]
7. Blackwell, T. Recent Demonstrations of Laser Power Beaming at DFRC and MSFC. In *AIP Conference Proceedings*; American Institute of Physics: Melville, NY, USA, 2005.
8. Yadav, K.; Kumar, B. Swaroop Mitigation of Mismatch Power Losses of PV Array under Partial Shading Condition Using Novel Odd Even Configuration. *Energy Rep.* **2020**, *6*, 427–437. [CrossRef]
9. Sprangle, P.; Hafizi, B.; Ting, A.; Fischer, R. High-Power Lasers for Directed-Energy Applications. *Appl. Opt.* **2015**, *54*, F201-9. [CrossRef]
10. AUVSI: LaserMotive, Lockheed Demonstrate Real-World Laser Power. Available online: https://www.flightglobal.com/auvsi-lasermotive-lockheed-demonstrate-real-world-laser-power/106546.article (accessed on 31 August 2025).
11. Nguyen, D.H. Dynamic Optical Wireless Power Transfer for Electric Vehicles. *IEEE Access* **2023**, *11*, 2787–2795. [CrossRef]
12. Hassija, V.; Saxena, V.; Chamola, V. Scheduling Drone Charging for Multi-Drone Network Based on Consensus Time-Stamp and Game Theory. *Comput. Commun.* **2020**, *149*, 51–61. [CrossRef]
13. Zhao, L.; Yao, Y.; Guo, J.; Zuo, Q.; Leung, V.C.M. Collaborative Computation Offloading and Wireless Charging Scheduling in Multi-UAV-Assisted MEC Networks: A TD3-Based Approach. *Comput. Netw.* **2024**, *251*, 110615. [CrossRef]

14. Montemanni, R.; Dell'Amico, M.; Corsini, A. Parallel Drone Scheduling Vehicle Routing Problems with Collective Drones. *arXiv* **2023**, arXiv:2307.03523. [CrossRef]
15. Yang, J.; You, X.; Wu, G.; Hassan, M.M.; Almogren, A.; Guna, J. Application of Reinforcement Learning in UAV Cluster Task Scheduling. *Future Gener. Comput. Syst.* **2019**, *95*, 140–148. [CrossRef]
16. Jin, Y.; Xu, J.; Wu, S.; Xu, L.; Yang, D.; Xia, K. Bus Network Assisted Drone Scheduling for Sustainable Charging of Wireless Rechargeable Sensor Network. *J. Syst. Arch.* **2021**, *116*, 102059. [CrossRef]
17. Nguyen, M.A.; Hà, M.H. The Parallel Drone Scheduling Traveling Salesman Problem with Collective Drones. *Transp. Sci.* **2023**, *57*, 866–888. [CrossRef]
18. Wang, X.; Poikonen, S.; Golden, B. The Vehicle Routing Problem with Drones: Several Worst-Case Results. *Optim. Lett.* **2017**, *11*, 679–697. [CrossRef]
19. Sacramento, D.; Pisinger, D.; Ropke, S. An Adaptive Large Neighborhood Search Metaheuristic for the Vehicle Routing Problem with Drones. *Transp. Res. Part C Emerg. Technol.* **2019**, *102*, 289–315. [CrossRef]
20. Das, D.N.; Sewani, R.; Wang, J.; Tiwari, M.K. Synchronized Truck and Drone Routing in Package Delivery Logistics. *IEEE Trans. Intell. Transp. Syst.* **2021**, *22*, 5772–5782. [CrossRef]
21. Deng, D.; Jing, W.; Fu, Y.; Huang, Z.; Liu, J.; Shimada, K. Constrained Heterogeneous Vehicle Path Planning for Large-Area Coverage. In Proceedings of the 2019 IEEE/RSJ International Conference on Intelligent Robots and Systems (IROS), Macau, China, 4–8 November 2019.
22. Jung, M.; Oh, H. Heterogeneous Mission Planning for a Single Unmanned Aerial Vehicle (UAV) with Attention-Based Deep Reinforcement Learning. *PeerJ Comput. Sci.* **2022**, *8*, e1119. [CrossRef]
23. Li, H.; Wang, H.; Chen, J.; Bai, M. Two-Echelon Vehicle Routing Problem with Time Windows and Mobile Satellites. *Trans. Res. Part B Methodol.* **2020**, *138*, 179–201. [CrossRef]
24. Wu, Q.; Zeng, Y.; Zhang, R. Joint Trajectory and Communication Design for Multi-UAV Enabled Wireless Networks. *IEEE Trans. Wirel. Commun.* **2018**, *17*, 2109–2121. [CrossRef]
25. Chowdhery, A.; Jamieson, K. Aerial Channel Prediction and User Scheduling in Mobile Drone Hotspots. *IEEE ACM Trans. Netw.* **2018**, *26*, 2679–2692. [CrossRef]
26. Liu, H.; Liu, T.; Huang, K. A Real-Time System for Scheduling and Managing UAV Delivery in Urban. *arXiv* **2024**, arXiv:2412.11590. [CrossRef]
27. Golden, B.; Raghavan, S.; Wasil, E.A. (Eds.) The Vehicle Routing Problem: Latest Advances and New Challenges. In *Operations Research/Computer Science Interfaces Series*, 2008th ed.; Springer: New York, NY, USA, 2008, ISBN 9780387777771.
28. Xu, W.; Wang, X.; Li, W.; Li, S.; Lu, C. Research on Test and Evaluation Method of Laser Wireless Power Transmission System. *EURASIP J. Adv. Signal Process.* **2022**, *2022*, 20. [CrossRef]
29. Balkan, N.; Erol, A. Light Emitting Diodes and Semiconductor Lasers. In *Graduate Texts in Physics*; Springer International Publishing: Cham, Switzerland, 2021; pp. 219–278. ISBN 9783319449340.
30. Zhang, Q.; Fang, W.; Liu, Q.; Wu, J.; Xia, P.; Yang, L. Distributed Laser Charging: A Wireless Power Transfer Approach. *IEEE Internet Things J.* **2018**, *5*, 3853–3864. [CrossRef]
31. Krupke, W.F. DPAL: A New Class of Lasers for Cw Power Beaming at Ideal Photovoltaic Cell Wavelengths. In *AIP Conference Proceedings*; American Institute of Physics: Melville, NY, USA, 2004.
32. Wang, X. Guizhou Power Grid Intelligent Operations Center Successfully Developed a UAV Remote Charging System. Available online: https://www.csg.cn/epaper/epaper/nfdwb/html/2024-11/26/content_4137.htm (accessed on 31 August 2025).
33. James, J.; Iyer, V.; Chukewad, Y.; Gollakota, S.; Fuller, S.B. Liftoff of a 190 Mg Laser-Powered Aerial Vehicle: The Lightest Wireless Robot to Fly. In Proceedings of the 2018 IEEE International Conference on Robotics and Automation (ICRA), Brisbane, Australia, 21–25 May 2018.
34. Wolsey, L.A.; Nemhauser, G.L. Integer and Combinatorial Optimization. In *Wiley Series in Discrete Mathematics and Optimization*, 1st ed.; John Wiley & Sons: Nashville, TN, USA, 2014, ISBN 9780471359432.
35. Babic, D. Piecewise Polynomial Approximation Based on Taylor Series with Efficient Realization Using Farrow Structure. In Proceedings of the 2009 9th International Conference on Telecommunication in Modern Satellite, Cable, and Broadcasting Services, Nis, Serbia, 7–9 October 2009.

Disclaimer/Publisher's Note: The statements, opinions and data contained in all publications are solely those of the individual author(s) and contributor(s) and not of MDPI and/or the editor(s). MDPI and/or the editor(s) disclaim responsibility for any injury to people or property resulting from any ideas, methods, instructions or products referred to in the content.